GROUND VORTEX FORMATION WITH TWIN JETS AND MOVING GROUND PLANE

K Knowles* and D Bray+

Royal Military College of Science, Shrivenham, UK

Abstract

The flow-fields associated with single and twin jets impinging in a cross-flow have been investigated experimentally and numerically. Parameters which affect the position and strength of the ground vortex have been investigated: nozzle height, nozzle pressure ratio, cross-flow-to-jet velocity ratio, vector angle and nozzle splay with both fixed and moving ground planes. Experimental results show that the ground vortex formed by an impinging jet in cross-flow moves away from the nozzle centre-line as cross-flow-to-jet velocity ratio is decreased; the rate of change of position, however, depends on other parameters. Increasing nozzle height above the ground causes little variation in vortex position for a single jet but a marked *forward* movement of ground sheet separation point in the case of twin jets. For all cases there is an increase in penetration with increasing nozzle pressure ratio up to choking, followed by a general reduction but with a second peak at pr=3. The effect of the moving ground plane is to reduce vortex penetration by about 24% on average. This suggests that a moving ground plane simulation (or moving model) is essential when testing design configurations in ground effect in wind-tunnels. It is also shown that rig design can produce a blockage effect which moves the ground vortex by up to 4 nozzle diameters - this can change other apparent parametric effects. The flow is seen to be very unsteady, especially in the presence of the twin jet fountain.

Nomenclature

A_n Nozzle exit area

C_p Pressure coefficient = $(p-p_\infty)/(\frac{1}{2}\rho_\infty V_\infty^2)$

d_n Nozzle exit diameter

h Height of nozzle exit above ground (see Fig. 2)

p Pressure

pr Pressure ratio = p_o/p_∞

T Thrust

V Velocity

V_e Effective velocity ratio = $\sqrt{\frac{1}{2}\rho_\infty V_\infty^2 / \frac{1}{2}\rho_1 w_1^2}$

w Jet velocity

y Horizontal distance measured upstream (ie against the crossflow) from nozzle centre-line (see Fig. 2)

δ Cross-flow boundary layer thickness

Δy_s y_s(short nozzle) - y_s(long nozzle)

ρ Density

Subscripts

c Maximum

g Groundplane

i Impingement (see Fig. 2)

n Nozzle

p Penetration (see Fig. 2)

s Separation (see Fig. 2)

v Vortex (see Fig. 2)

∞ Ambient (cross-flow)

o Nozzle stagnation conditions

1 Jet exit conditions

* Lecturer, Aeromechanical Systems Group. MRAeS, MAIAA.
+ Lecturer, Aeromechanical Systems Group. MRAeS

Introduction

When a jet impinges on a surface normal to its axis a wall jet is formed which spreads out radially from the impingement point. If a cross-flow (parallel to the wall) exists then the wall jet will eventually stagnate and roll up to form a vortex, arranged as a horse-shoe about the jet (Fig. 1). This flow-field is of particular interest in the development of advanced short take-off and vertical landing (ASTOVL) aircraft, where the cross-flow may be due to ambient wind or aircraft motion. With twin jets there is the added complexity of the fountain formed by the two opposing wall jets.

The position and strength of the ground vortex are important due to their effects on aircraft pressure loads and air intake flows (where there is the specific problem of hot gas ingestion - HGI). Some of the factors which affect the ground vortex position have been investigated previously[1-4] but there is

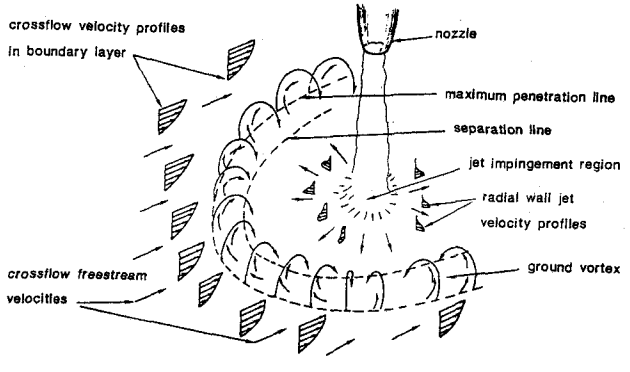

Fig.1 Ground vortex formed by impinging jet in cross-flow

considerable scatter in the experimental data and very little high jet Mach number data. There seem to be no data on the factors which affect the forward penetration of the wall jet formed by twin impinging jets. The present project has looked at the influence of nozzle height (2 to 8 nozzle diameters), nozzle pressure ratio (1.05 to 4), cross-flow-to-jet velocity ratio (0.1 to 0.01) and vector angle (-5 to +10 degs) for single- and twin-jet configurations with both fixed and moving ground planes (simulating ambient wind or aircraft motion). For the twin-jet configurations the effect of nozzle splay is also being investigated.

Operationally, the current flow-field is of interest in two cases: hovering in cross-wind near the ground and the so-called rolling vertical landing (RVL) in which the aircraft maintains some forward motion as it lands. Combinations of the two could also occur. Simulating the first case is relatively straightforward as this can involve a fixed nozzle above a fixed ground plane in a wind-tunnel - provided that the atmospheric boundary layer is satisfactorily modelled, which may involve artificially thickening the tunnel wall boundary layer. Simulation of an RVL is more complex. One solution is to use a moving model but this can entail mechanical complexity and impose limitations on the testing envelope. An alternative is the use of a rolling road in a wind-tunnel - an arrangement often used for ground vehicle aerodynamics.

A two-dimensional view of the ground vortex flow-field is shown in Fig. 2. This represents conditions in the plane of symmetry for a single, normally-impinging jet in cross-flow. In this plane the static pressure along the ground would vary as shown in Fig. 3. This reveals three quantifiable positions relating to the ground-vortex: the maximum penetration point, y_p (also referred to as the stagnation point), the separation point, y_s, and the vortex core position, y_v. For the present work the surface static pressure distribution has been measured (using a static probe just above the ground) and the position y_p or y_s used to quantify wall jet forward penetration. This contrasts with the flow visualisation approach taken by many previous investigators and discussed in Ref. 5. Flow visualisation has also been used in the present work and results from the two techniques have been compared. Other work discussed in Ref. 5 is that of Green[6] and Stott[7] who worked in collaboration with the present authors and used the static pressure plotting technique developed here to conduct a parametric investigation into a single, normally-impinging jet in cross-flow. These previous investigations are summarised in Fig. 4 and discussed in more detail in Ref. 5. It should be noted that, although y_s is used in this figure, smoke flow visualisation experiments are likely to produce a penetration which is closer to y_p.

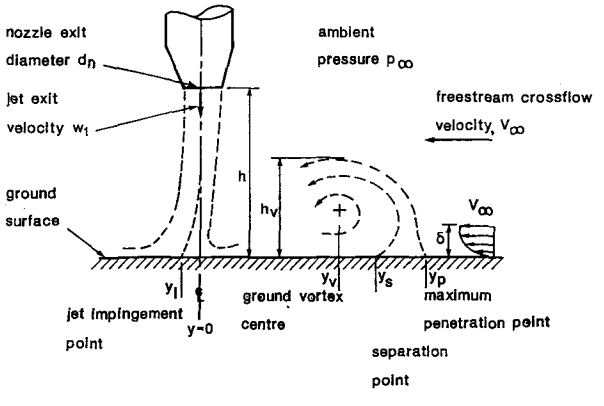

Fig.2 Plane of symmetry for single impinging jet in cross-flow

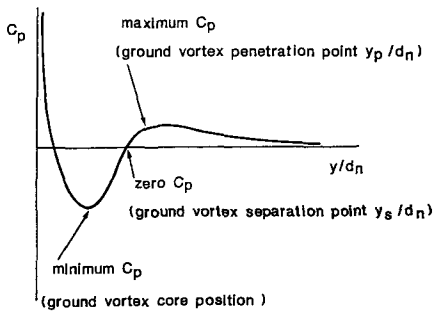

Fig.3 Typical ground vortex static pressure distribution

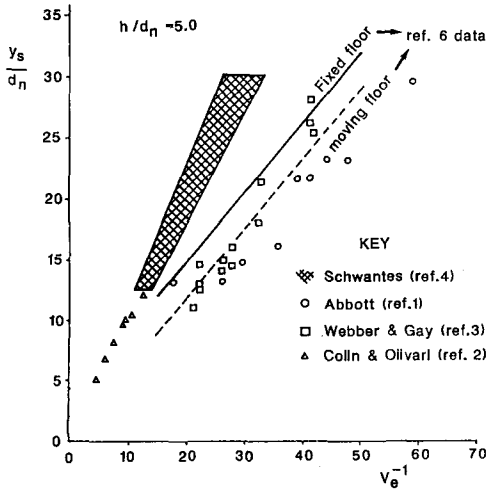

Fig.4 Normalised vortex penetration against effective velocity ratio - comparison of previous investigations

Experimentation

A schematic of the experimental layout is shown in Fig. 5. The RMCS open-jet wind-tunnel (OJWT), having a 1.1 x 1.5m elliptical nozzle, supplies the cross-flow with a maximum wind speed of 42ms^{-1}. In the working section is a removable "rolling road" (1.1 x 1.7m) with a boundary layer suction slot upstream. To prevent the rolling road belt from flapping or lifting off its base, belt suction is provided. This is arranged in four separate full-span sections; the level of suction in each section can be varied independently. It is thus possible to increase the belt suction under the forward part of the vortex (where considerable "lift" was experienced) whilst suction is reduced under the impingement point. Evenso, the combination of lift under the front of the vortex and a large download under the jet impingement can provide a limit to the test conditions available with the rolling road on, especially if large nozzles are used.

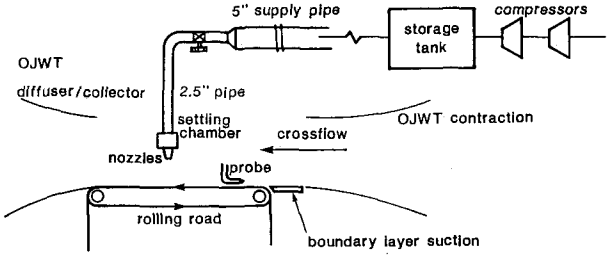

Fig.5 RMCS experimental rig schematic

Compressed air for the jets is provided by two "Howden" screw-type compressors which can either be run in series (to give a maximum flow rate of $0.9kgs^{-1}$ at 7bar) or in parallel ($1.8kgs^{-1}$ at 4bar). The air is dried and then dumped into a $34m^3$ storage tank. The ambient-temperature air is then supplied through a 5in (12.7cm) diameter pipeline which is reduced to 2.5in before reaching the wind-tunnel working section. In the tunnel the pipe is connected to a settling chamber (approx. 34cm wide, 14cm deep and 15cm high, externally) to the lower surface of which one or two nozzles can be fitted. By incorporating different designs of lower plate nozzle vector (fore and aft angle) and splay or toe-in (differential transverse angle) can be incorporated. When comparing vectored and un-vectored test results it should be noted that the perpendicular height (in nozzle diameters) from the ground plane to the centre of the nozzle exit planes was the same in each case. Similarly, with different splay (or toe-in) angles the distance between the two nozzle centre-lines at exit was maintained at three diameters.

The nozzles initially adopted for these tests were of conical, convergent design, having a 1in (25.4mm) exit diameter (d_n), a 0.25in-long contraction of 10^o semi-angle and a parallel section upstream of this. The total nozzle length was $5d_n$. Since the ground vortex position depends on d_n it became necessary, for many test conditions, to use smaller nozzles with d_n=0.5in. These were non-dimensionally the same as the 1in nozzles, in an attempt to produce similar exit conditions, and are referred to here as the "short half-inch" nozzles. The lower settling chamber heights above the ground plane involved in using these short nozzles were found to produce unacceptable blockage effects. Consequently, 0.5in-diameter nozzles, of length $10d_n$, were adopted (the "long half-inch" nozzles). It is not felt that any change in nozzle exit velocity profile resulting from the use of these longer nozzles would affect the overall flow-field significantly - as demonstrated by previous results[5].

Nozzle pressure ratio was determined from the measurement of settling chamber static pressure (provided by four tappings around the perimeter manifolded together). Ground plane static pressures were measured using a Pitot-static tube aligned with the cross-flow and traversed in the streamwise direction. Ground plane static pressures were referenced to local jet-off static pressures to account for the slight streamwise pressure gradient along the tunnel. For the single jet tests the traverse plane was the plane of symmetry of the horseshoe vortex. For the twin nozzle cases traverses were conducted both in this plane of symmetry (half-way between the two nozzles) and in a parallel plane through one nozzle centre-line. The probe was mounted on a traversing rig and positioned as close as possible to the ground surface (typically 4mm to the centre-line of a 4mm-diameter probe), without being noticeably affected by any ground belt flapping. This "stand-off probe" technique has been validated by comparison with fixed ground board static tappings[5]; the only measureable errors involved are under the ground vortex[6,7] where, as expected, the probe gives a lower static pressure. The positions of y_p, y_s and y_v, however, are not significantly affected by the use of the probe.

The range of test conditions is shown in Table 1 for the present experiments. Earlier results with a single 30^o convergent nozzle and no settling chamber were reported previously[5]. An important parameter in comparing test results has been found to be the cross-flow velocity ratio:

$$V_e = \sqrt{\tfrac{1}{2}\rho_\infty V_\infty^2 / (\tfrac{1}{2}\rho_1 w_{c_1}^2)}$$

For choked, convergent nozzles w_{c_1} presents some difficulty in evaluation. Whilst the exit velocity for such nozzles is sonic, use of this value for w_{c_1} would make no allowance for the different jet flow-fields produced at different under-expanded pressure ratios. For the present work w_{c_1} is defined as the velocity which would exist at the exit of a fully-expanded convergent-divergent nozzle operated at the same pressure ratio as our convergent nozzle. An alternative value can be calculated based on thrust, thus:

$$w_{c_1} = \sqrt{\frac{T}{2\rho_1 A_n}}$$

where T can either be measured[6,7] or calculated using a 1-D assumption. (It should be noted that Refs. 6 and 7 define their effective velocity ratio as $V_e^{-1} = w_{c_1}/V_\infty$). It has previously been shown[5,8] that this latter definition appears to lead to poorer data collapse when plotting against V_e. The "fully-expanded" value of w_{c_1} is, therefore, preferred here.

Table 1 Values of test parameters

pr_n[a]	h/d_n	V_∞[b] (ms^{-1})	V_∞[c] (ms^{-1})	Vector angle[d] (deg)	Splay angle[e] (deg)
1.05	2	2.6	10.3	-5	+10
1.8	4	3.9	15.4	+5	-10
3.0	8	5.1	20.6	+10	-20
4.0					

a Extra tests at pr_n=1.5, 2.5 for single, normal nozzle only.
b At pr_n = 1.05 only.
c At all pr_n except 1.05.
d See Fig. 14 for sign convention.
e Positive splay ≡ jets diverging.

Results and discussion

The results of much of the present work can be presented in terms of vortex penetration as a function of one of several parameters. The authors have previously quantified vortex penetration by using y_p. As discussed in Ref.8, however, there appears to be a constant relationship between y_p (or y_v) and y_s, as shown in Fig. 6; furthermore, Ing and Bailey[9] suggested that y_s is to be preferred because its determination is less susceptible to experimental error. For the present work y_s will generally be used to quantify vortex penetration; the corresponding value of y_p can be determined from Fig. 6.

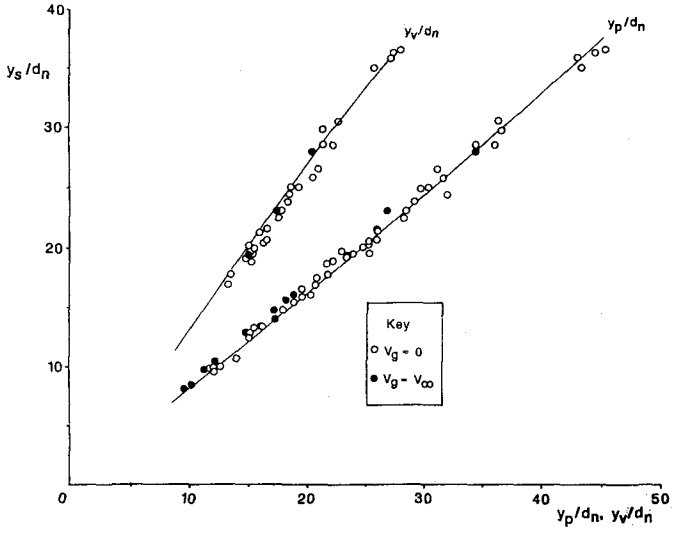

Fig.6 Ground-vortex self-similarity

It was mentioned earlier that using a nozzle with d_n=0.5in and a length of $5d_n$ (the "short half-inch" nozzle) produced a tunnel blockage effect. This can be quantified by plotting non-dimensional separation distance for a short nozzle against that for a long nozzle (under the same conditions). The effect was most pronounced at low nozzle heights (h/d_n=2) as shown in Fig. 7. The blockage does not produce a consistent increase in separation distance (Fig. 8) - errors varied between a maximum increase in separation distance of 30% (h/d_n=2, pr_n=1.8, V_e^{-1}=16) and a maximum reduction of 5% (h/d_n=8, pr_n=4.0, V_e^{-1}=76). There appears to be a maximum absolute increase in y_s for an effective velocity ratio in the region of 20 to 30 with a tendency towards a reduction in y_s once V_e^{-1} exceeds 50 to 70. Whilst no explanation is offered for these effects it is clear that varying blockage must be borne in mind when comparing results from different rigs. The present results also emphasise the need for accurate representation of full-scale conditions in tests on this flow-field.

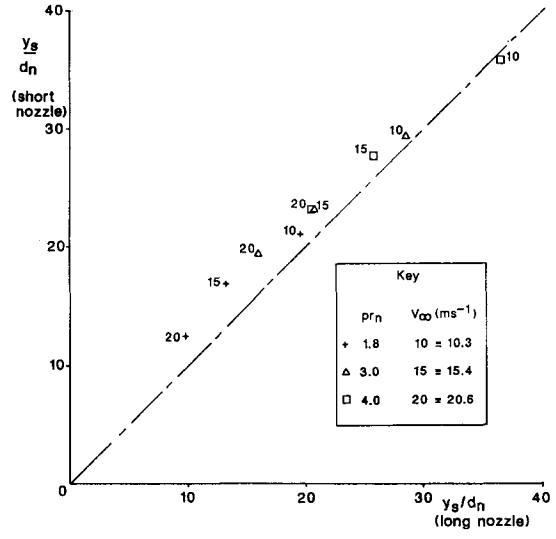

Fig.7 Rig blockage effect (single nozzle, h/d_n=2, V_g=0)

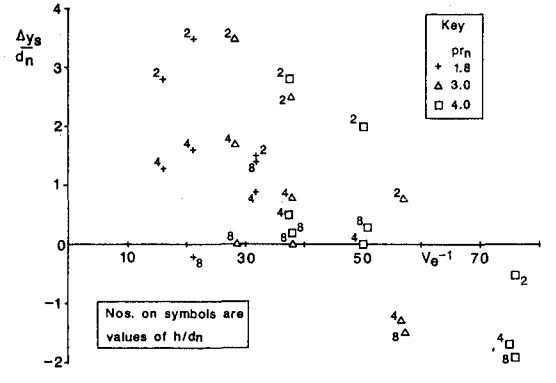

Fig.8 Blockage effect as a function of effective velocity ratio (single nozzle data)

1. Single nozzle results

1.1 Effect of V_e and V_g

As expected, and shown previously (Fig. 4), reducing cross-flow velocity (increasing V_e^{-1}) causes an increase in vortex penetration (Fig. 9). The rate of change of y_s (or y_p) with V_e, however, depends on other test conditions, as discussed below. This could account for some of the data spread shown in Fig. 4, as could the use of moving, rather than fixed, models (or ground planes) and the different flow visualisation techniques.

The present tests confirm[5-9] that the use of a rolling road simulation consistently produces a reduction in vortex penetration compared with the fixed ground plane, as shown in Figs. 9 and 10. This reduction, which on average is 24%, is presumably due to the reduction in cross-flow momentum deficit produced by using the rolling road (Fig. 11) and/or the increased wall jet shear stress. Which of these, if either, is the dominant effect is not clear: experiments elsewhere suggest that changes in cross-flow boundary layer thickness (of the order of a few nozzle diameters) do not affect vortex formation[10]; large boundary layer thicknesses, however, do cause an increase in vortex penetration[8,9]. From the point of view of wind-tunnel model tests on ASTOVL configurations, the mechanism by which the vortex penetration changes is not of immediate importance; what is important is that an RVL must be simulated using a rolling road or moving model.

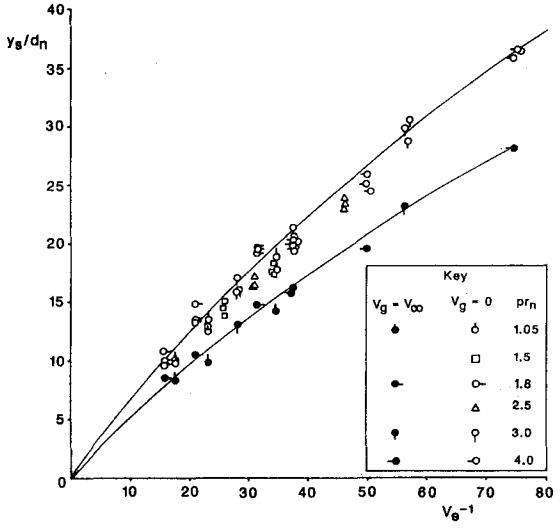

Fig.9 Separation distance vs. effective velocity ratio (long 0.5in single nozzle)

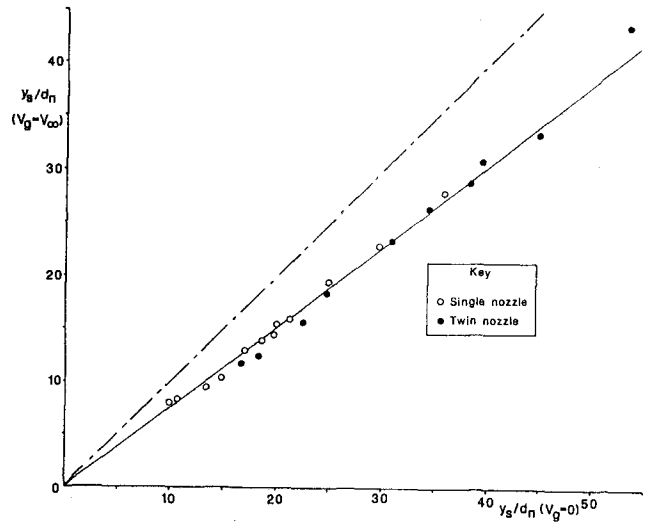

Fig.10 Effect of rolling-road on separation distance (long 0.5in nozzles)

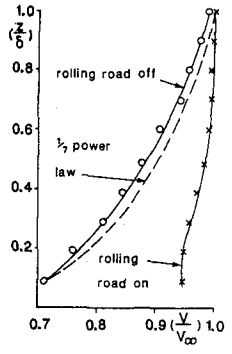

Fig.11 Effect of rolling-road on cross-flow boundary layer profile (V_∞=15ms^{-1}, traverse at y=.105m)

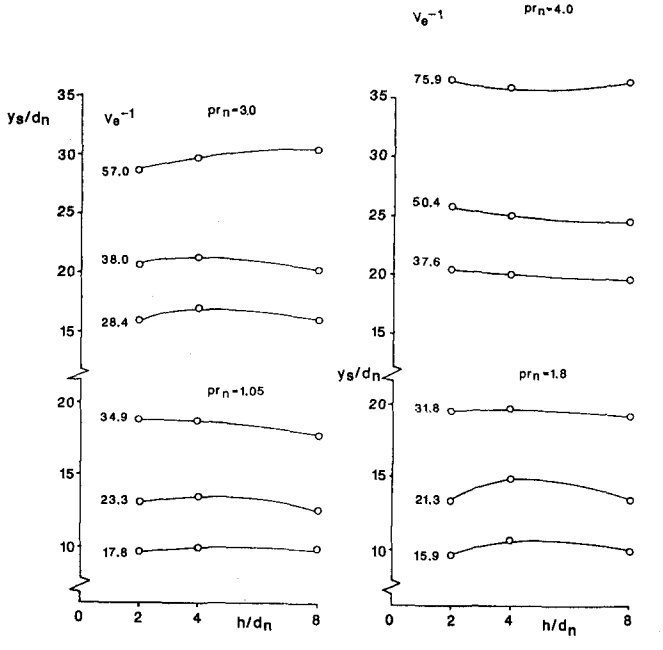

Fig.12 Effect of height on separation distance (long 0.5in single nozzle)

1.2 Effect of nozzle height

It has previously been suggested that vortex penetration can increase with increasing nozzle height[4], although this is not a consistent trend[9] and the most recent work using pressure plotting[6,7] does not show movements which are very significant compared with the general experimental uncertainty[5]. The present results tend to confirm the view that (within the current range) there is little consistent effect of nozzle height (Fig. 12). The slight height effects shown by the work of Green[6] and Stott[7] and discussed earlier[5,8,9] might largely be accounted for by blockage effects. The trends shown are an increase in penetration of the order of $3\text{-}4d_n$ for height changes between 2.5 and $10d_n$ (additional tests at h/d_n=15 did not show a consistent further increase). The current "short half-inch" nozzle tests showed a maximum over-penetration of a similar order. This demonstrates that rig blockage can cause vortex movements of the same order of magnitude as the "height effect" measured previously; it does not explain the earlier results because the trends are in the wrong direction. However, the rig used by Green and Stott, although similar in concept to that used here had some important differences: upstream and downstream fairings on the settling chamber and a much wider nozzle (approximately $3d_n$ external width, compared with $1.5\text{-}2d_n$ for the present nozzles). The nose fairing is particularly important since it extends approximately $11d_n$ forward of the nozzle centre-line. This will almost certainly influence the vortex flow-field (even for y_s of the order of $20d_n$) and, in this case, may cause an under-penetration of the vortex at low rig heights. If the variation of vortex penetration with nozzle height can be explained as largely a blockage effect then that would seem far more satisfactory than invoking an "increase of momentum" due to increased entrainment[4]. Furthermore, it is important from the point of view of wind-tunnel testing to note that the influence of nozzle height on vortex position can be rig-dependent.

1.3 Effect of nozzle pressure ratio

One of the reasons behind the use of the current experimental facility for studying this impinging jet flow-field was the ability to determine the effect of different jet Mach numbers, in the range of operational interest, separately from the effect of V_e. This latter can be varied in water tunnel test facilities where it is easier to obtain good LDA flow-field mapping[11] but it was necessary here to quantify nozzle pressure ratio effects.

As discussed in Ref. 5, the results of Stott[7] show a general, although not consistent, trend with pressure ratio. This general trend is for penetration to increase as pressure ratio increases from 1.5 to 3, followed by a decrease, or little change, in penetration up to pr_n=4. The present results (Fig. 13) show a consistent trend (albeit over a more limited range of conditions than Stott's): penetration increases up to choking, decreases up to pr_n=2.5, peaks again at pr_n=3 and then levels off or further reduces slightly. This is, at least, consistent with the changes in shock pattern which occur over this pressure ratio range (Ref. 12), but is markedly different from the trends shown by Stott[7]. Part of the explanation seems to lie in the definitions of w_{c_1} and V_e. Stott uses measured thrust to calculate an equivalent w_{c_1} which is then ratiod directly with V_∞, whereas we use a fully-expanded velocity and ratio the square roots of dynamic pressures. Thus, at pressure ratios of 3 and 4 Stott has a lower value of V_e^{-1} than in the present work, for the same conditions. His curves therefore jump from a low V_e^{-1} (say 40) in Fig. 13 to a higher value (say 50) at pr_n=3. At low vortex penetrations there is also the likelihood of rig interference effects in the results of Ref. 7.

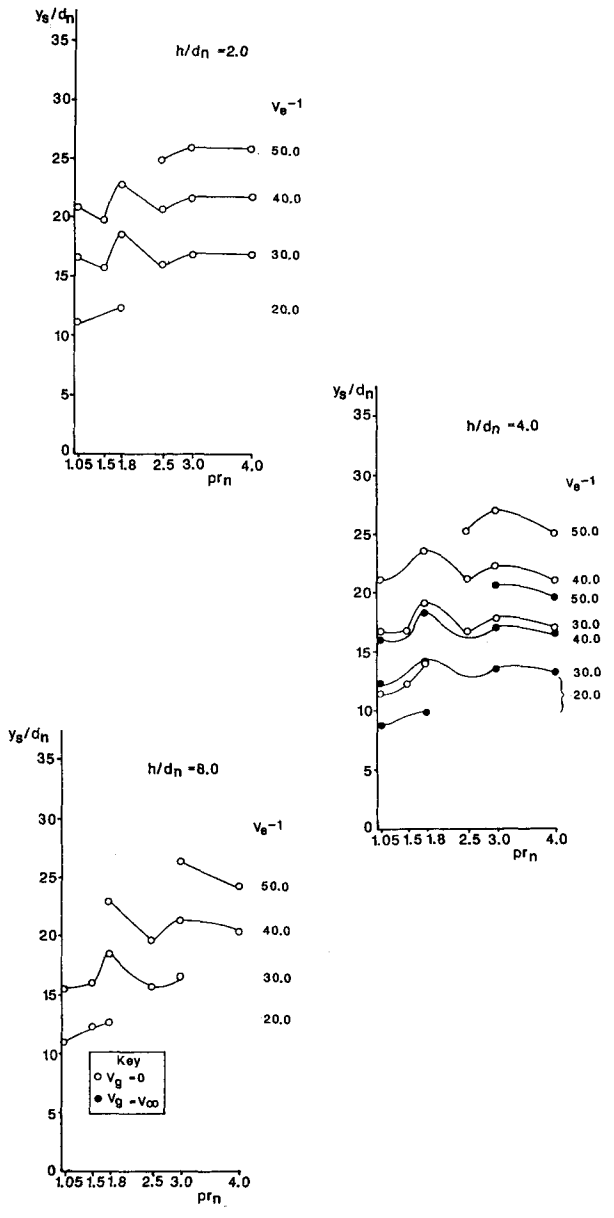

Fig.13 Effect of pressure ratio on separation distance (long 0.5in single nozzle)

1.4 Effect of nozzle vector angle

The effect of vectoring the nozzle is shown in Fig. 14. Three vector angles have been considered, -5^o, $+5^o$, $+10^o$, the sign convention being indicated on the figure. In each case the origin for y is the intersection of the nozzle centre-line with the ground plane. A forward vector of -5^o causes an increase in penetration of about 15%, with a rearward vector of $+5^o$ giving a similar decrease, compared with the normal impinging jet. 10^o rearward vector gives a 23% reduction in penetration. (The trend lines indicated in Fig. 14 are for the single nozzle results only.) Note that the vortex self-similarity is not affected by vectoring - vectored results are plotted in Fig. 6 as well as non-vectored cases. It is assumed that the effect of the rolling road is uniformly additive to that of nozzle vector.

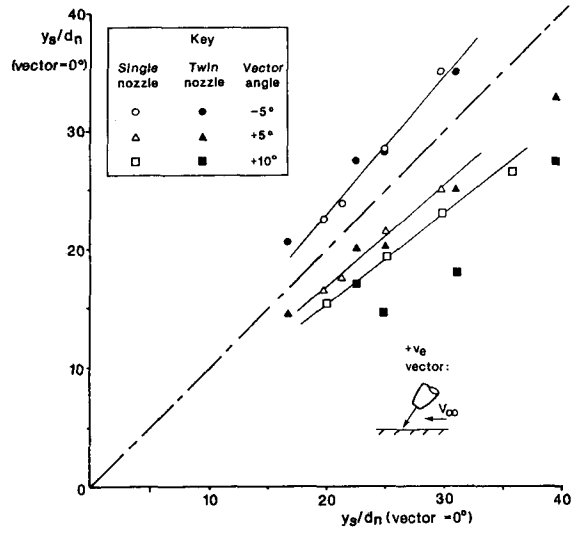

Fig.14 Effect of vector angle on separation distance (long 0.5in nozzles)

2. Twin nozzle results

Static pressure traverses conducted in the twin nozzle plane of symmetry revealed a similar distribution to that found in the single nozzle cases but with no minimum C_p detected within the traverse range (Fig. 15). Similar results were obtained in the parallel traverse plane through one nozzle centre-line. Whether this is due to probe errors or indicates no ground vortex, a weak vortex or a vortex outside the traverse range is not immediately clear, although this last option is unlikely due to vortex self-similarity (see below). It should also be recognised that the plane of symmetry, especially close to the nozzles, already contains a separated shear layer (the fountain) and that within this sheet static pressures are sub-atmospheric[13]. The absence of an apparent vortex does not prevent separation and penetration distances (y_s and y_p) being quantified. When plotted on the same basis as Fig. 6 the same self-similarity is revealed as for the single nozzle. Thus, it is unlikely that there is a vortex outside the traverse range.

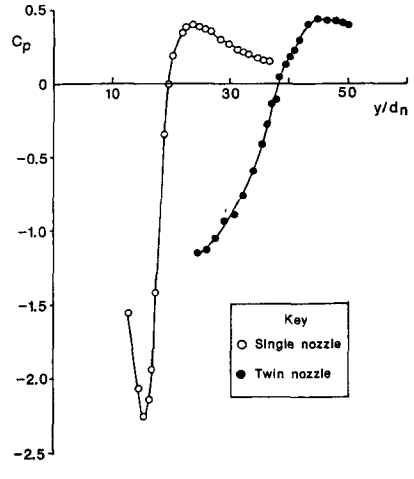

Fig.15 Static pressure distributions in the plane of symmetry (long 0.5in nozzles, pr_n=1.8, h/d_n=4, V_∞ =10.3ms^{-1}, V_g=0, vector=0^o)

All results currently available from our twin (side-by-side) nozzle tests are shown in Fig. 16 where they are compared with the equivalent single nozzle cases (i.e. the same h/d_n, pr_n, V_e). It can be seen that, on average, forward penetration is almost doubled, although there tends to be a greater increase at higher y_s (up to 114%) and less at lower penetrations (40%). Such a direct comparison between twin and single nozzles is not, however, particularly meaningful due to the increased nozzle exit momentum from the twin nozzles. Thus, a better comparison would be between the twin nozzles and a single nozzle of the same total exit area, i.e. of exit diameter $\sqrt{2}d_n$. This comparison can be achieved by non-dimensionalising y_s for the twin nozzles by $\sqrt{2}d_n$, which results in a twin-nozzle penetration 40% (on average) greater than that for a single nozzle of equal exit area. It should be noted, however, that the twin nozzle arrangement has over 40% more jet surface area (at nozzle exit) than the equivalent single nozzle. At low penetrations (y_s less than about $10d_n$) the twin nozzle data tend towards the equivalent single nozzle penetrations.

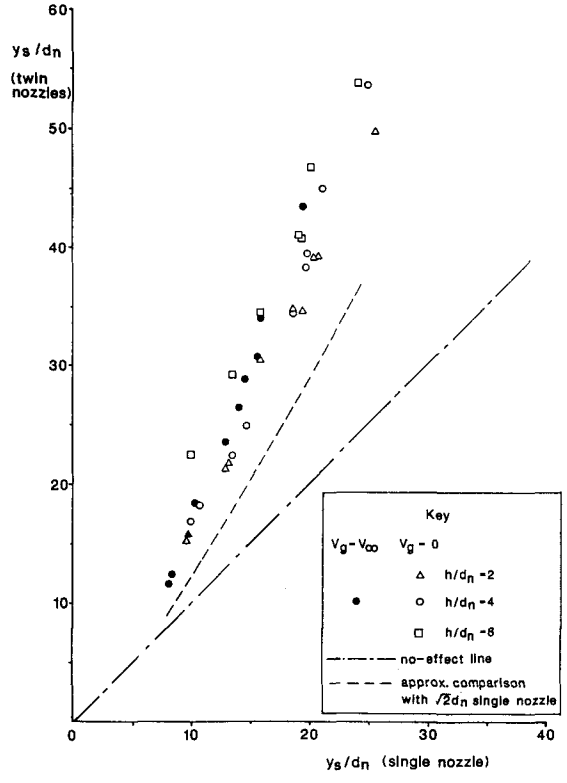

Fig.16 Comparison of twin nozzle and single nozzle separation distances (long 0.5in nozzles)

2.1 Effect of V_e and V_g

The same general trend with V_e is seen with twin nozzles as was the case for the single nozzle. As shown in Fig. 16, however, penetration is increased with twin nozzles even over that expected of a single nozzle of the same total exit area. The effect of the rolling road is almost identical with twin nozzles to that found with a single nozzle. The data collapse onto the same line, showing a reduction in penetration of 24% (Fig. 10).

2.2 Effect of nozzle height

The current twin nozzle tests have shown a marked and fairly consistent trend of increasing penetration with increasing nozzle height above the ground (Fig. 17). Over the height range of 2 to $8d_n$, these penetration increases vary between only 1 diameter at pr_n=4, V_e^{-1}=37.76, to 10 diameters at pr_n=1.05, V_e^{-1}=34.9, but with all the other cases showing an increase of penetration between 4 and $8d_n$. This is generally a bigger change in penetration than would seem to be explained by the blockage effect discussed earlier (although there is more nozzle cross-sectional area in the flow than with a single nozzle). It is not clear exactly what is the mechanism causing this effect; it may be associated with the fountain flow, in which case nozzle spacing may also have an influence. For the current spacing of $3d_n$ and assuming a jet spreading angle of 7° (the spreading rate of the $w_c/2$ line deduced from Ref. 12), simple geometry suggests that the two jets will start to merge at about $8d_n$. As discussed below, merging of the jets seems to produce increased penetration.

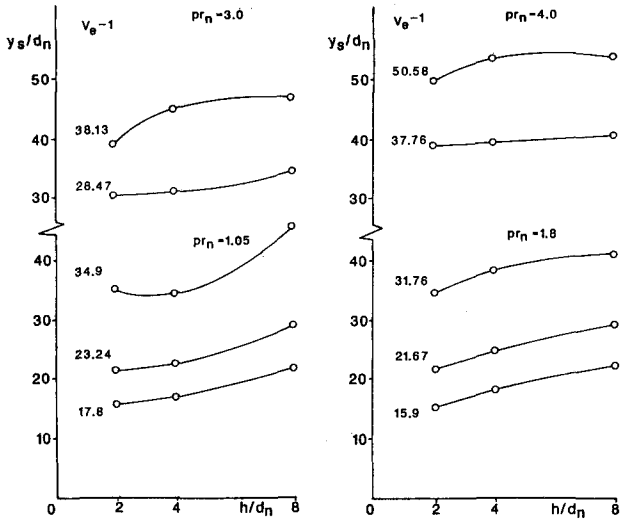

Fig.17 Effect of height on separation distance (long 0.5in twin nozzles)

2.3 Effect of nozzle pressure ratio

Very similar pressure ratio effects are seen with twin nozzles as were noted with the single nozzle. There is an increase in penetration up to choking followed by a levelling-off or decrease. The only significant difference occurs at the highest height tested where there is relatively little increase in penetration up to choking.

2.4 Effect of nozzle vector angle

The twin nozzle vector results are shown in Fig. 14. For 5° vector, the twin nozzle configuration shows very similar trends to those for the single nozzle. The results for +10°, however, show more under-penetration and far less linear behaviour than the single nozzle. There appears to be a "kink" in all the twin-nozzle trends at a non-vectored separation distance of $22-25d_n$; either side of this the twin nozzle data tend to run parallel with those for the single nozzle. What might be causing this is not clear, nor are there enough data points to be sure that it is a significant trend.

2.5 Effect of nozzle splay

So far nozzle splay has only been investigated using flow visualisation[14] (see below). Three angles are being tested: 10° of nozzle centre-line divergence; 10° of centre-line convergence and 20° of convergence. For each configuration trends with h/d_n and V_e have been considered; pressure ratio effects could not be studied because of rig limitations. Further work currently in hand is looking at these effects (including that of pr_n) using the probe traverse techniques described above. For the toed-in nozzles the flow visualisation has shown a maximum penetration at a particular height; $h=4d_n$ for the 10° toe-in case and $2d_n$ for 20°. These are very close to the jet merging heights predicted from the jet spreading rates discussed in section 2.2 ($3.27d_n$ and $1.96d_n$ respectively). This would tend to support the view that as the jets merge and the fountain disappears there is an increase in ground sheet penetration.

3. Flow visualisation studies

The single and twin impinging jet flow-fields have been investigated using smoke flow visualisation. This study used a separate, smaller-scale rig from that used for the pressure traverse work. Air was supplied from a portable compressor to single or twin 10mm-diameter pipes; these discharged to atmosphere, without further contraction, in the open working section of a small (0.76m diameter) wind tunnel. Exit velocities from the 10mm pipes were of the order of $50ms^{-1}$, or less[14]. Upstream of these pipes a venturi was formed in a wider-bore section and smoke injected through a centre-line nozzle.

Initial flow visualisation used a horizontal laser light sheet with a video camera in a forward-scatter position[15]. For quantitative measurements, however, it was felt that a normal viewing angle was needed. The camera was therefore mounted directly above the ground board, in which position the laser light sheet proved ineffective so flood-lighting was adopted. A fixed ground plane was used on which a reference grid was marked. The tunnel contraction was faired in to the plate leading edge to avoid separation there. The full range of conditions (except pr_n and V_g) covered by the pressure traverse tests was investigated, as well as the splay tests discussed above. Comparisons between the two techniques show reasonably good agreement (based on y_p). For the single nozzle the largest difference in penetration is $2d_n$, with a uniform scatter of data except at $h/d_n=8$ where the flow visualisation consistently gives more penetration. For the twin nozzle tests there is more data scatter (up to $5d_n$) and $h/d_n=8$ data all show a reduced penetration.

The main use of the flow visualisation tests has been to reveal the ground vortex unsteadiness, which is generally increased by the presence of a fountain flow (quantifying this unsteadiness is the object of a further phase of this work), and to show the extent to which the fountain sheet projects forward of the rest of the ground vortex. It is noted that, at least at low values of V_e^{-1} (about 16), the locus of the rest of the ground vortex is very similar for both single and twin jets under the same conditions.

4. Numerical modelling

The flow-field for a single, normally-impinging jet in cross-flow has been modelled numerically using the commercially-available, finite-volume code PHOENICS. The initial development of the modelling was described in Ref. 16 and an extensive discussion of the current work is given in Ref. 17. Only 2-D, axisymmetric modelling has been undertaken so far, using the $k-\epsilon$ turbulence model with standard values for the model parameters. Despite this simplistic modelling it is interesting to note which of the effects discussed above can be predicted.

Using a grid of 49 by 51 around 10 hours of cpu time on a VAX 8700 were required for satisfactorily-converged solutions. This model is found to be able to produce a similar flow-field to that observed experimentally, in terms of velocity vectors and ground plane pressure coefficient distribution (Fig. 18). Vortex geometry is reasonably accurately predicted, i.e. the relative values of y_v, y_s, and y_p. The absolute value of y_s is, however, over-predicted (by around $7d_n$ for a given V_e). This is primarily attributed to the 2-D modelling which forces the cross-flow out of the solution domain through the upper free surface, thus reducing the horizontal component of cross-flow momentum available for stagnating the wall jet. The rate of increase of vortex penetration with V_e^{-1} is, however, well predicted.

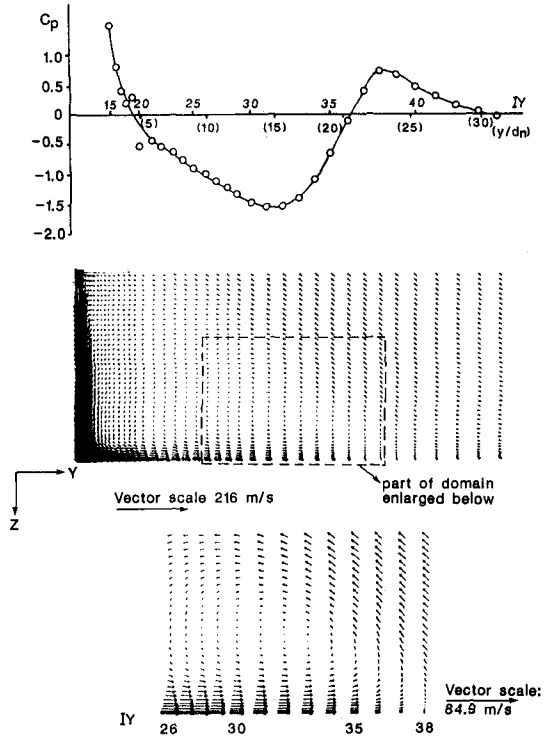

Fig.18 2-D PHOENICS calculation: flow-field vectors and corresponding ground-plane Cp distribution.

The numerical results show a consistent relationship between y_s and h: in all cases y_s reduces slightly with increasing nozzle height, typically by $1.3d_n$ for $h/d_n=2.5$ to 10. This is believed to be due to inaccuracies in the free jet turbulence modelling when using the unmodified model coefficients. These lead to over-predicted axial velocity decay rates, with the over-prediction tending to increase with increasing h/d_n.

The modelling shows the correct trend with moving ground plane operation, although the reduction in separation distance is under-predicted (12% against 24% observed experimentally). This under-prediction is again believed to be due to the free jet turbulence modelling inaccuracies discussed above. These lead to incorrectly predicted wall jet profiles and, hence, under-predicted wall jet shear stresses with the ground plane moving.

Nozzle pressure ratios of 1.05, 1.2, 1.5 and 2.0 have been modelled to date. The correct trends are shown (increasing y_s with increasing pr_n) but the rate of increase seems to be over-predicted (typically $5d_n$ over this pr_n range). It is hoped to extend this work to moderately and highly under-expanded jets using an up-dated version of the PHOENICS code offering superior shock-capturing. Work is also in hand to extend the modelling to 3-D calculations for single and twin jets.

Conclusions

An experimental investigation has been made into the parameters which affect the position of the ground vortex formed by single and twin impinging jets in cross-flow. It has been confirmed that there is a constant relationship between the penetration distance, the separation distance and the position of the vortex core, thus, any one of these can be used to quantify ground sheet forward penetration. In terms of y_s the following trends have been found.

- Penetration increases with increasing V_e^{-1}.
- Penetration decreases when a moving ground plane is used, whether this is primarily due to reduced cross-flow momentum deficit or increased wall jet shear stress is not yet clear.
- There appears to be no effect of nozzle height for single jets and previous results showing an effect are thought to be rig-dependent.
- There is an increase of penetration with height for twin jets and this seems to be associated with the two jets merging.
- Penetration increases with nozzle pressure ratio (at constant V_e) up to choking, it decreases at higher pressure ratios but with a second, lower peak around pr_n=3.
- Vectoring the nozzles forwards increases penetration (relative to the geometric impingement point) and rearward vectoring gives a reduction: 15% for 5^o and 23% for 10^o.
- Using twin nozzles gives a greater penetration than an equivalent single nozzle, although flow visualisation suggests that this is confined to the central, upwind portion of the ground sheet.
- Preliminary investigations of nozzle splay (non-parallel centre-lines) suggest that peak penetrations occur when the two jets start to merge.

Simple numerical modelling of the single jet flow-field has shown most of these parametric trends correctly. Experimentally, the current studies have found the flow-field to be extremely unsteady, especially in the presence of the twin-jet fountain flow. Further work is planned to quantify this unsteadiness as well as to investigate other parametric effects and to extend the computations.

Acknowledgement

The authors wish to thank British Aerospace, Military Aircraft Ltd and, in particular, Mr P Curtis and Mr P G Knott for their help with the current work. Much of this work has been funded by BAe.

References

1. Abbott, W A, "Studies of flow fields created by vertical and inclined jets when stationary or moving over a horizontal surface", Aero. Res. Council, CP no. 911, Oct. 1964.

2. Colin, P E and Olivari, D, "The impingement of a circular jet normal to a flat surface with and without cross-flow", European Research Office, AD 688-953, Jan. 1969.

3. Webber, H A and Gay A, "VTOL reingestion model testing of fountain control and wind effects", AIAA paper no. 75-1217, AIAA/SAE 11th Propulsion Conf., Sept./Oct. 1975.

4. Schwantes, E, "The recirculation flow pattern of a VTOL lifting engine", NASA TT F-14912, June 1973.

5. Bray, D and Knowles K, "Normal impinging jet in crossflow - a parametric investigation", AIAA paper no. 89-2957, AIAA/ASME/SAE/ASEE 25th Joint Propulsion Conf., Monterey, CA, July 1989.

6. Green, L, "Phase 1 jet in crossflow and ground effect tests in the Warton 5.5m low speed wind tunnel", rept. no. BAE-WWT-RP-RES-AXR-189, British Aerospace plc, Nov. 1988.

7. Stott, M R, "Phase 2 jet in crossflow and ground effect tests in the Warton 5.5m low speed wind tunnel", rept. no. BAE-WWT-RP-RES-AXR-196, British Aerospace plc, Nov. 1988.

8. Knowles, K, Bray, D, Bailey, P J and Curtis, P, "Impinging jets in cross-flow", Int. Powered Lift Conf., London, Aug, 1990.

9. Ing, D and Bailey, P J, "Model RA117 - data analysis of phase 2 jet in cross-flow and ground effect tests in the Warton 5.5m low speed wind tunnel", Logico Systems Ltd. rept. no. 18, June 1989.

10. McGuirk, J J, private communication, Imp. Coll., London, Mech. Eng. Dept., 1989.

11. Barata, J M M, Durao, D F G and McGuirk, J J, "Numerical study of single impinging jets through a crossflow", J. Aircraft, 26, 11, Nov. 1989, pp 1002-8.

12. Donaldson, C du P and Snedeker, R S, "A study of free jet impingement, part 1, mean properties of free and impinging jets", J. Fluid Mech., 45, 2, pp. 281-319, 1971.

13. Abbott, W A and White, D R, "The effect of nozzle pressure ratio on the fountain formed between two impinging jets", RAE Tech. Memo. P 1166, May 1989.

14. Tidball, I C, "V/STOL aerodynamics", RMCS 42 degree course Aero. Eng. project rept., May 1990.

15. Power, J, "V/STOL aerodynamics - development of experimental facilities", RMCS 41 degree course Mech. Eng. project rept., May 1989.

16. Knowles, K and Bray, D, "High Mach number impinging jets in cross-flow - comparison of computation with experiment", in: "Numerical Methods in Laminar and Turbulent Flow" vol. 6, ed. Taylor, C. et al., pp. 1389-1398. Pub. Pineridge Press, Swansea, 1989.

17. Bray, D and Knowles, K, "Numerical modelling of impinging jets in cross-flow", AIAA paper no. 90-2246, AIAA/ASME/SAE/ASEE 26th Joint Propulsion Conf., Orlando, Florida, 16-18 July, 1990.